HUNTINGTON MEDICAL RESEARCH INSTITUTES
NEURAL ENGINEERING LABORATORY
734 Fairmount Avenue
Pasadena, California 91105

Contract No. N01-NS-1-2340
Quarterly Progress Report
April 1 - June 30 2002
Report No.3

"Functional Microstimulation of the Lumbosacral Spinal Cord"

Douglas McCreery, Ph. D.
Albert Lossinsky, Ph.D.
Victor Pikov, Ph.D
Leo Bullara, B.A.
William Agnew, Ph.D.

ABSTRACT

The objective of this project is to develop neuroprostheses that will allow patients with severe spinal cord injuries to regain control of their bladder and bowel. The approach is based on an array of microelectrodes that is implanted into the sacral spinal cord. An array of 9 discrete iridium microelectrodes was implanted into the rostral S_2 spinal cord of cat SP131. The tips of these electrodes were slightly sharper (radius of curvature of 2-3 ：m vs 5-6 ：m in previous animals) to determine if this would affect the gliotic scarring that frequently occurs ventral to the tips sites. A silicon-substrate array with 6 shanks and 12 electrode sites was implanted at the rostral S_2 level of cat SP132.

Urodynamic measurements were obtained from cat Sp131 at 23, 43 and 70 days, and from cat SP132 at 42 and 68 days after implanting the arrays. At both post-implant times, and in both cats, an elevation in bladder pressure and relaxation of the urethral sphincter, and also micturition, could be elicited by pulsing with selected electrodes.

For chronic stimulation (SP131), the cat was lightly anesthetized with Propofol and we used stimulus parameters which had induced relaxation of the urethral sphincter during the urodynamic measurements. Two electrodes were pulsed for a total of 24 hours (12 hrs/day) on two successive days. The stimulus waveform was cathodic-first, controlled-current, charge-balanced (biphasic) pulse pairs, 100 ：A in amplitude and 400 ：s in duration, at 20 Hz. The charge per phase was 40 nC, the charge density was 2,000 ：C/cm². The pulse frequency was 20 Hz with a 10% duty cycle (1 minute of stimulation; 9 minutes without stimulation repeated indefinitely). At the end of the 2nd day, the cat was deeply anesthetized and perfused with fixative for histologic evaluation of the electrode sites. Cat SP132 did not receive stimulation, since the objective was to determine if the sharper electrodes affected the severity of the gliotic scarring beneath the tip sites.

The silicon array implanted into cat SP131 continued to function throughout 73 days *in vivo.* The histologic evaluation of the implant site revealed no evidence of old or recent hemorrhages near any of the 6 silicon shanks. The shanks were surrounded by a sheath of connective tissue that was somewhat thicker (approximately 25 ：m) than is typical of the discrete iridium shafts, but along most of the length of the shafts, there were viable neurons within 50-100 ：m of the track. There was a noticeable reduction in the density of NeuN-positive neurons around the tips of all 6 shanks. This does not appear to reflect a loss of neurons but rather a reduction in the expression of the NeuN protein. The phenomenon does not appear to be related to insertion trauma, since the actual glial scarring extended only about 100 ：m below the tip sites.

The array of 9 discrete iridium microelectrodes in cat SP132 was implanted for 71 days, at the junction of the S_1 and S_2 levels. These electrodes were slightly sharper (tip radius of curvature = 2.5-3.0 ：m) than in previous animals (tip radius of curvature = 5-6 ：m). We have consistently observed gliotic scars extending for several hundred microns below the blunter tips, and we have hypothesized that this may be due to micro impact trauma during electrode implantation. Indeed, there was no evidence of these scars in cat SP132. However, the interpretation of the findings from this animal is complicated by the fact that this array did not insert fully, and thus, the electrodes did not penetrate as deeply into the spinal cord.

The tips of electrodes 1, 2 and 3 were in the dorsal part of the intermediate horn, about midway between the sacral parasympathetic nucleus and the central canal and pulsing with these electrodes produced a transient increase in bladder pressure, but no appreciable relaxation of the urethral sphincter. The tips of electrodes 7, 8 and 9 were in the ventral part of the dorsal columns, just dorsal to the dorsal grey commissure. Stimulation through any of these produced a marked relaxation of the urethral sphincter. Stimulation with electrode 9 also produced a marked increase in bladder pressure.

The tips of electrodes 4, 5 and 6 were in, or very close to, the intermediolateral cell column which contains the cell bodies of the sacral parasympathetic nucleus. Thus, stimulation through these electrodes produced an increase in bladder pressure. However, the stimulation also produced contraction of somatic muscles of the hindlimbs. This probably was due to spread of current into the ventral horn which, at this level (caudal S_1), contains the " motor neurons that enervate the muscles of the pelvic floor and the perigenital region.

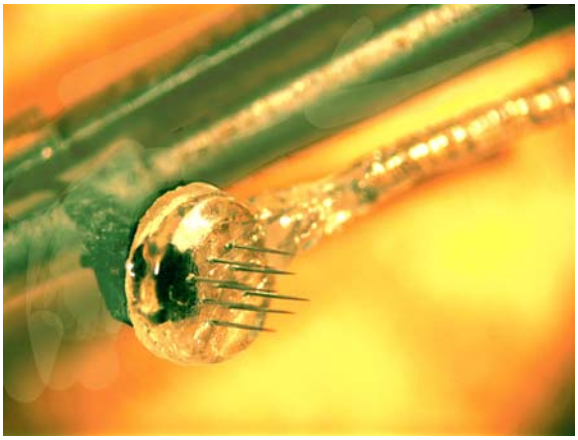

Figure 1

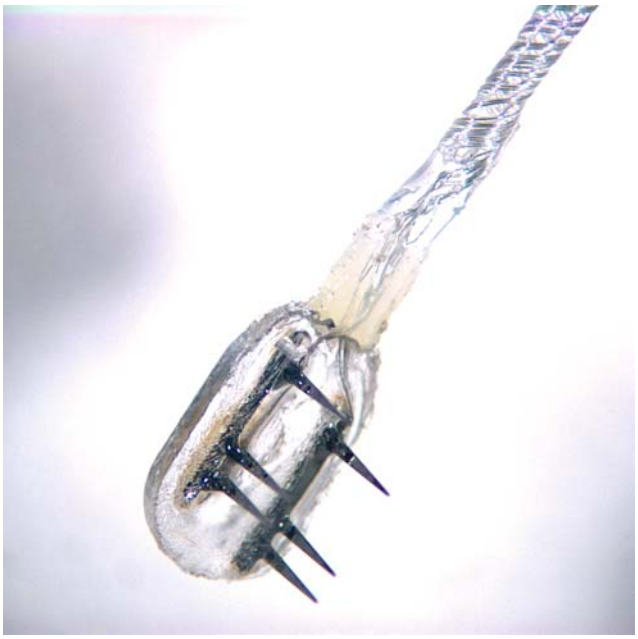

Figure 2

METHODS

The objective of this project is to develop neuroprostheses that will allow patients with severe spinal cord injuries to regain control of their bladder and bowel. The system is based on an array of microelectrodes that is implanted into the sacral spinal cord. The procedures and hardware are being developed in cats with intact spinal cords, and in the 2nd year of the project, the implanted cats will undergo transection of the spinal cord at the low thoracic level.

Fabrication and implantation of the arrays

An array of 9 discrete iridium microelectrodes was implanted into the rostral S_2 spinal cord of cat SP132 (Figure 1). The tips of these electrodes were slightly sharper (radius of curvature of 2-3 ：m vs 5-6 ：m in previous animals) to determine if this would affect the severity of the gliotic scarring that frequently occurs ventral to the tips sites. A silicon-substrate array with 6 shanks and 12 electrode sites was implanted at the rostral S_2 level of cat SP131 (Figure 2).

To locate the S_2 cord level, we stimulated the perigenital skin, and recorded at each of several locations along the dorsal surface of the sacral cord. The arrays were implanted near the maximum of the 2nd component of the evoked response (the dorsal cord potential). At autopsy, the position of the array was validated by complete dissection of the spinal roots. The arrays were inserted int the spinal cord with the high-speed inserter tool at a velocity of approximately 1 m/sec. The dura was then closed over the array, using 5 pre-installed sutures.

Urodynamic measurements of hydrostatic bladder pressure and infusion pressure within the EUS were obtained at intervals after implantation. During this procedure, the cats were anesthetized lightly with Propofol. The apparatus used for these measurements has been described previously (QPR #1, #2).

At 72 days after implantation of the array, cat SP131 was anesthetized with Propofol and 2 of the electrode sites (1 and 2) on the silicon array were pulsed for 12 hours on each of two successive days. The electrodes were pulsed with biphasic, charge-balanced, controlled-current pulsed, at 100 ：A, 400 ：s/phase (40 nC/phase) at 20 Hz, and with a 10% duty cycle (60 second on, 540 second off, repeated). Cat SP132 did not receive stimulation, since the objective was to determine if the sharper electrodes affected the severity of the gliotic scarring beneath the tip sites.

Histologic Procedures

Cats SP131 and SP132 were deeply anesthetized with pentobarbital, given i.v. heparin and perfused through the aorta for 30 seconds with a prewash solution consisting of ca. 250 ml of phosphate-buffered saline, and 0.05% procaine HCL. The animals were perfused with 4 L of a fixative containing 4% formalin and 0.25% glutaraldehyde in 0.1 M sodium phosphate buffer. Fixation of the spinal cord was good and the electrode arrays were determined in both cats to be within the caudal portion of S_1 and the rostral portion of S_2.

Tissue blocks containing both the microelectrodes and areas rostral and caudal to the electrodes were held in 0.1 M phosphate buffer, dehydrated in a graded series of ethanol and embedded in paraffin. The paraffin-embedded tissue blocks containing the electrode tips were cut at a thickness of 6-7 : m and 4 sections were picked up on each histogrip-coated-slide. Electrode tips were located in unstained sections. The group of slides containing the electrode tips were stained for the NeuN neuron-specific protein, with Nissl counterstain or Nissl alone in an alternating pattern. This allowed each electrode tip to be evaluated using both stains. The NeuN antibody recognizes many vertebrate neuron-specific proteins within the nuclei (primarily) and neuronal cytosol (to a slightly lesser degree) within the CNS. Histologic sections were photographed using a SPOT Insight digital microscope camera with 1600 x 1200 pixel resolution.

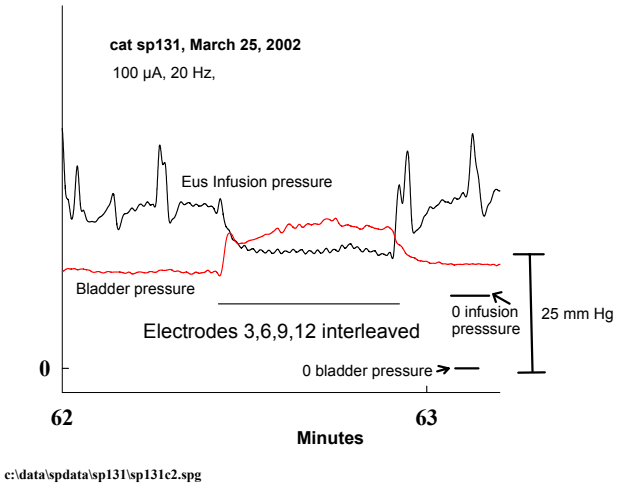

Figure 3A

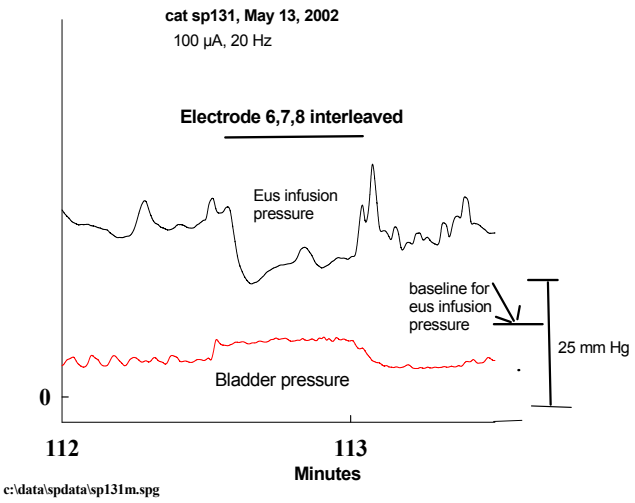

Figure 3B

RESULTS

Measurements of bladder and sphincter pressure

Urodynamic measurements were obtained from cat Sp131 at 23, 43 and 70 days, after the implant surgery. Figure 3A shows the hydrostatic pressure in the urinary bladder and the infusion pressure in the external urethral sphincter at 23 days after the implant surgery. Figure 3B shows the corresponding measurements at 70 days after implantation. Between the 23 and 70th day, the efficacy of the various electrodes changed, and the stimulation would induce only a small increase in bladder pressure. However at both times marks, interleaved pulsing of a selected

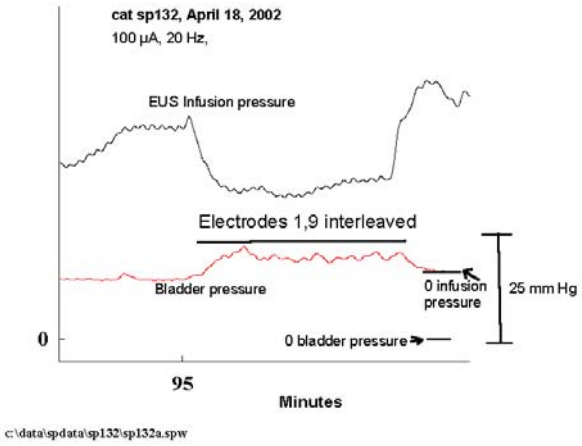

Figure 4A

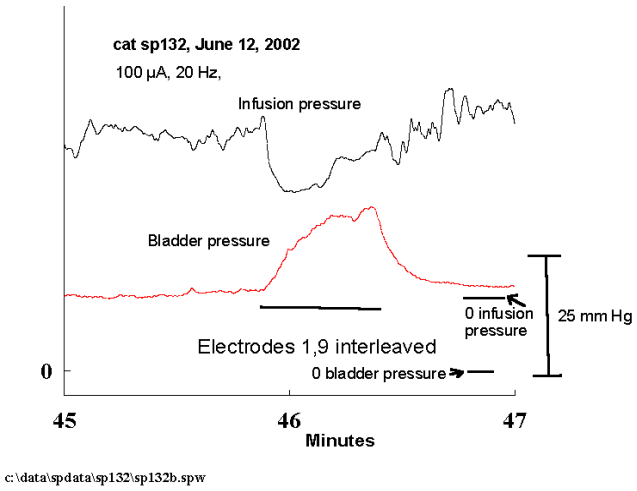

Figure 4B

combination of electrodes (3,6,9) at 23 days, and 6,7,8 at 70 days) induced micturition.

Urodynamic measurements were obtained from cat SP132 at 42 and 68 days after the implant surgery. Figure 4A shows the hydrostatic pressure in the urinary bladder and the infusion pressure in the external urethral sphincter at 42 days after the implant surgery. Figure 4B shows the corresponding measurements at 68 days after implantation. In this case, the combination of electrodes 1 and 9 was most effective in eliciting micturition, at 42 and at 68 days.

Cat SP131 was sacrificed for histologic evaluation at 73 days after implantation of the array, immediately after the two-day stimulation. Cat SP132 (which did not receive chronic stimulation) was sacrificed at 72 days.

Histologic Findings

Cat SP131 was sacrificed for histologic evaluation at 73 days after implantation of the array. Cat SP132 (which did not receive stimulation) was sacrificed 72 days after implantation. In both cats the electrode tips were located in the S_1 - S_2 spinal cord regions. There were no hemorrhages. With the exception of a few leukocytes close to one pulsed electrode site in SP131, remarkable inflammatory foci were not observed in either animal. There was minimal neovascularization in association with all tracks of the discrete iridium microelectrodes and the silicon shanks.

SP131. The silicon substrate electrode array in SP131 reached deep into medial portion of the ventral horns (Figures 5-10). There was a thickened capsule surrounding one of the two stabilizing shanks (Figure 10). This capsule was composed primarily of astroglia and fibroblasts.

There was limited gliotic scarring in the region ventral to tips (Figure 9). The brown colored HRP-DAB reaction product specific for the NeuN protein revealed the distribution of the neurons and their processes (Figures 5-10). The density of neurons and their processes surrounding all of the shanks appeared reduced (Figures 5-10).

SP132. In this animal, the tip sites of the 6 outboard iridium microelectrodes were located either within the middle or in the lateral portions of the dorsal horns (Figures 11-13). The tips of the three central electrodes were located within the dorsal white column, above the central canal (Figures11-16). There was evidence of limited lateral movement of electrode 6 in this animal, as revealed by an angulated gliotic scar (Figure 12). However, gliotic scaring ventral to the electrode tips was not observed. New or resolved hemorrhages were not observed and there was minimal neovascularization surrounding the nine electrode tracks (Figure 14). Only a few scattered leukocytes were observed in association with the electrode tip sites. The distribution of neurons adjacent to the six electrode tips within the dorsal gray horns were best evaluated at low magnification using NeuN immunohistochemistry (Figures 11-13). Nissl staining revealed several neurons that appeared to be undergoing chromatolysis (Figure 17A). Adjacent NeuN-stained sections indicated that they were NeuN-positive, albeit a weaker reaction (Figure 17B).

DISCUSSION

We have completed the first trial of a fully functional silicon substrate intraspinal microstimulating array (cat SP131). The results have been quite encouraging. The array continued to function throughout 73 days *in vivo.* The histologic evaluation of the implant site revealed no evidence of old or recent hemorrhages near any of the 6 silicon shanks. The shanks were surrounded by a sheath of connective tissue that was somewhat thicker (approximately 25 ：m) than is typical of the discrete iridium shafts, but along most of the length of the shafts, there were viable neurons within 50-100 ：m of the track. There was a noticeable reduction in the density of NeuN-positive neurons around the tips of all 6 shanks. This does not appear to reflect a loss of neurons but rather a reduction in the expression of the NeuN protein. It may be a consequence of the mechanical stress and strain induced by small, repeated movements of the rigid electrode tips within the much softer spinal cord. The phenomenon does not appear to be related to insertion trauma, since the actual glial scarring extended only about 100 ：m below the tip sites. One observation does suggest that when a neuron is stressed or injured, it does stain less darkly for the NeuN antibody; neurons undergoing chromatolysis, with diffuse Nissl substance, eccentric nuclei and a swollen appearance were less darkly stained for NeuN. Because of this staining variability, we are in the process of developing methods for quantitation of neuronal cell populations using NeuN immunohistochemistry.

An array of 9 discrete iridium microelectrodes was implanted for 71 days into the sacral cord of cat SP132. These electrodes were slightly sharper (tip radius of curvature 2.5-3.0 ：m) than in previous animals (tip radius of curvature 5-6 ：m). We have consistently observed gliotic scars extending for several hundred microns below the blunter tips, and we have hypothesized that this may be due to micro impact trauma during electrode implantation. Indeed, there was no evidence of these scars in cat SP132. However, the interpretation of the findings from this animal is complicated by the fact that this array did not insert fully, and thus, the electrodes did not penetrate as deeply into the spinal cord. We will continue to evaluate the sharper electrodes. We

did not pulse any of the electrodes in cat SP132, and we have yet to determine if the greater nonuniformity of current density associated with the sharper tips will make them more prone to erosion and spalling of the iridium oxide.

In cat SP132, the correlation between the tip sites and the physiologic responses is interesting. The array was in caudal S_1 and rostral S_2, and the tips of electrodes 1, 2 and 3 were in the dorsal part of the intermediate horn, about midway between the sacral parasympathetic nucleus and the central canal. Pulsing with these electrodes produced a transient increase in bladder pressure, but no appreciable relaxation of the urethral sphincter. The tips of electrodes 7, 8 and 9 were in the ventral part of the dorsal columns just dorsal to the dorsal grey commissure. Stimulation through any of these electrodes produced a marked relaxation of the urethral sphincter as would be predicted on the basis of their location. Surprisingly, stimulation with electrode 9 also produced a marked increase in bladder pressure. This may have been due to excitation of the preganglionic parasympathetic neurons of the intermediolateral cell column by depolarizing their dendrites, many of which pass close to the site of these electrode tips. Indeed, when electrodes 1 and 9 were pulsed together in the interleaved mode, the combination produced a marked increase in bladder pressure and a relaxation of the urethral sphincter.

The tips of electrodes 4, 5 and 6, were in, or very close to, the intermediolateral cell column which contains the cell bodies of the sacral parasympathetic nucleus. Thus, stimulation through these electrodes produced an increase in bladder pressure. However, the stimulation through electrodes 4 or 5 also produced contraction of somatic muscles of the hindlimbs. This probably was due to spread of current into the ventral horn which, at this level (caudal S_1), contains the " motor neurons that enervate the muscles of the pelvic floor and the perigenital region.

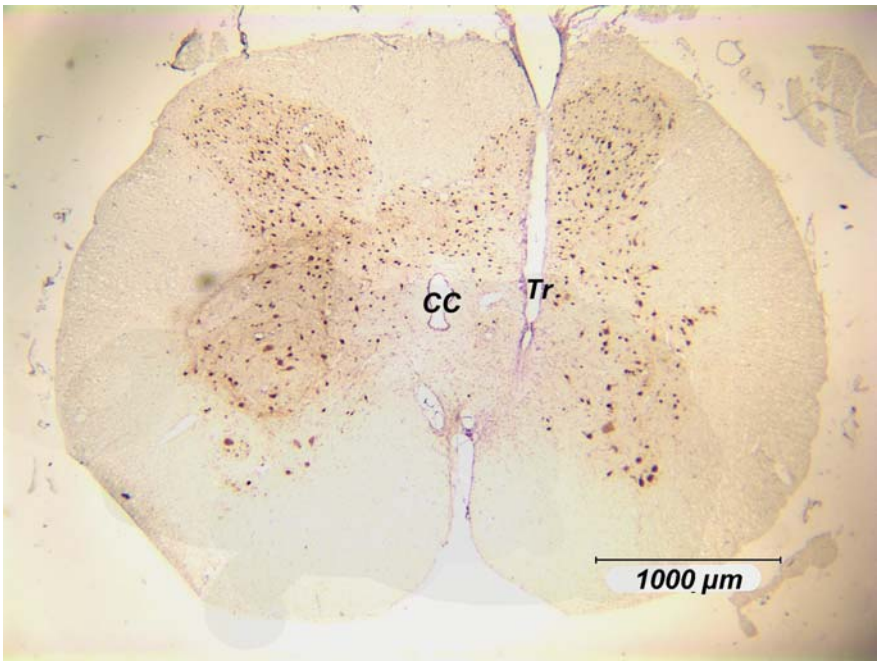

Figure 5. SP131, Silicon Shank 1. This low magnification view shows the tract (Tr) of the electrode capsule. Note the brown colored NeuN-positive neurons and neuronal processes primarily within the gray matter. The density of NeuN staining is reduced near the tip of the track. The central canal (CC) is also shown. There are no hemorrhages. NeuN-peroxidase

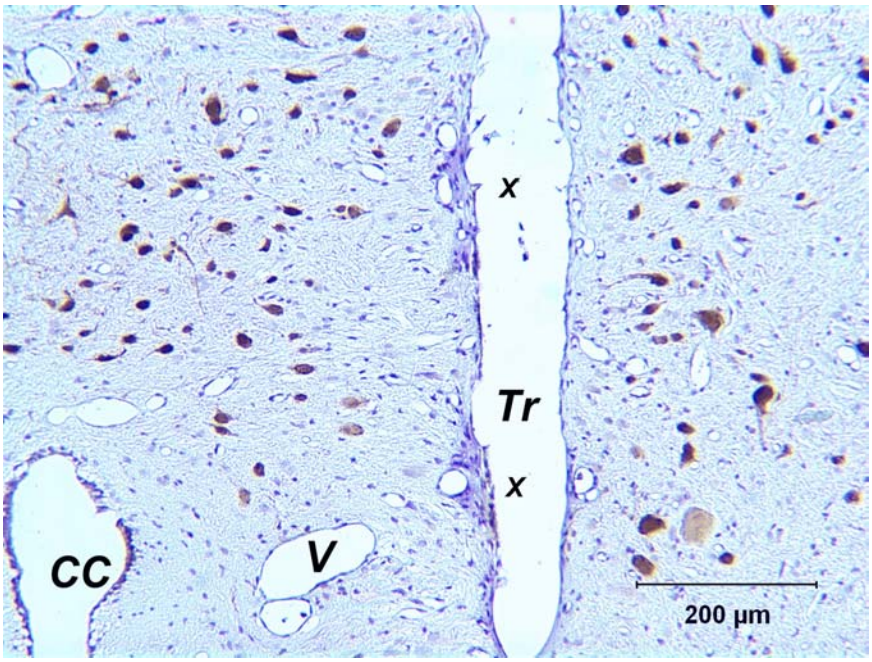

immunoreaction with Nissl counter stain.

Figure 6. SP131, shank 1, with two pulsed electrode sites (X). A few leukocytes are close to the pulsed sites, suggesting a mild inflammatory response. Brown NeuN-positive neurons and neuronal processes, thin-walled blood vessels (v) and the central canal (CC) are shown. NeuN-peroxidase Immunoreaction with Nissl counter stain.

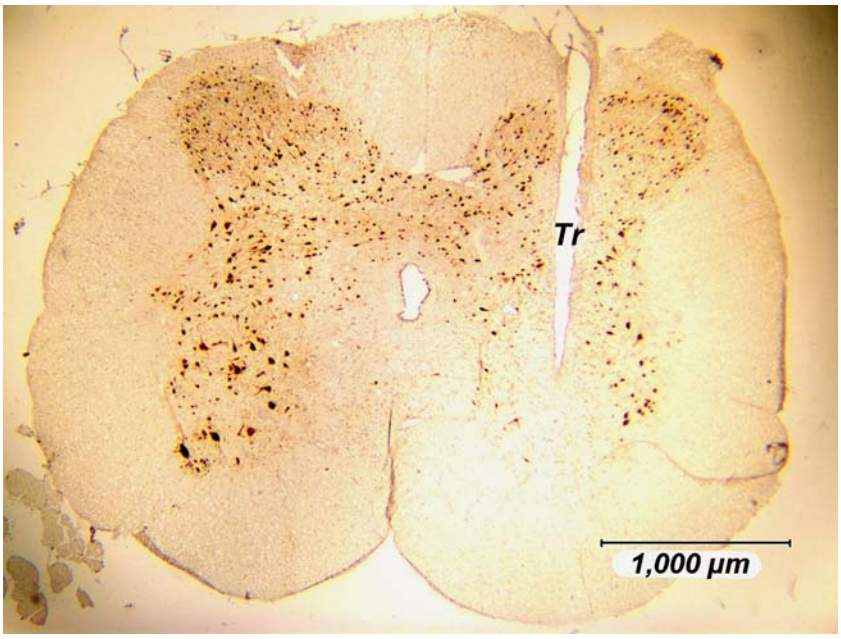

Figure 7. SP131, Shank 3. Low magnification view shows the capsule surrounding the track of the shaft (Tr). Note the reduced number of brown-colored, NeuN-positive neurons near the tip of the shank, compared to the contralateral side of the cord. Hemorrhages are not present. NeuN-peroxidase immunoreaction with Nissl counter stain.

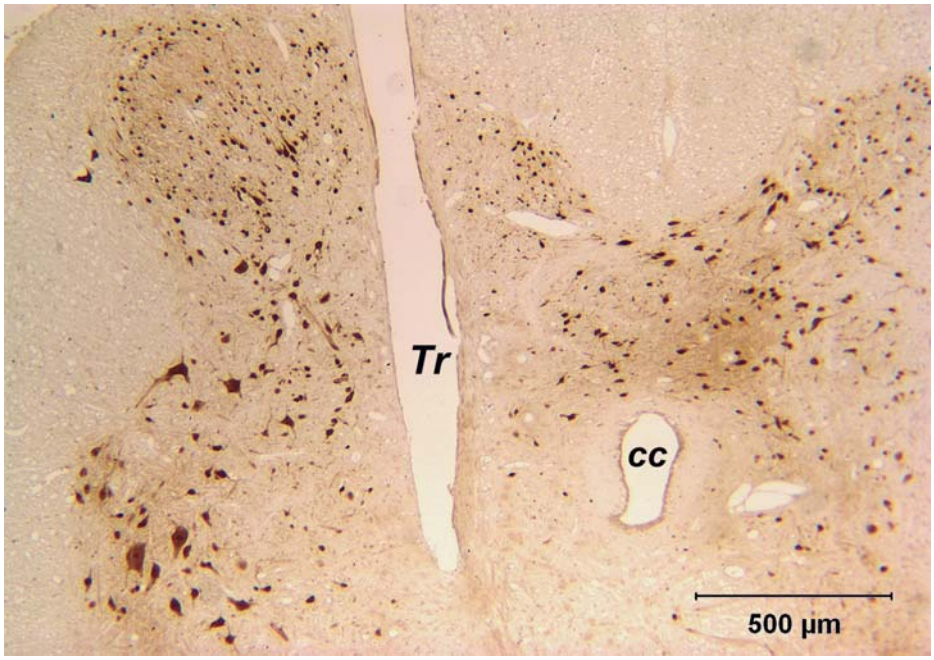

Figure 8. SP131, Shank 3. Note the reduced number of brown colored, NeuN-positive neurons and neuronal processes near the tip of the shank's track. The central canal (CC) also is shown. NeuN-peroxidase immunoreaction with Nissl counter stain.

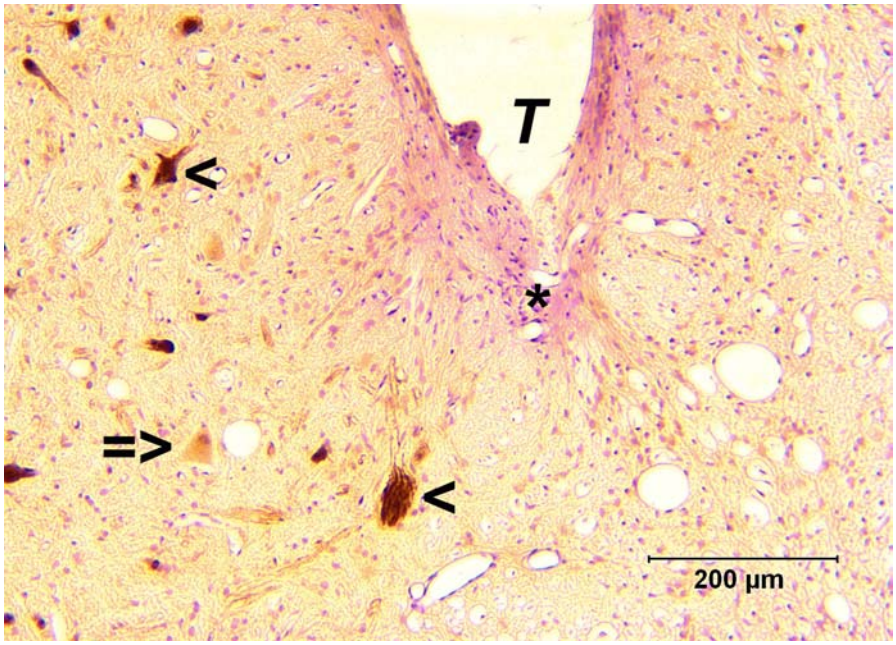

Figure 9. SP131, Tip site (T) of stabilizing shank 1. Note the differentiation between the brown-colored NeuN-positive neurons and neuronal processes (**<**), and the magenta-colored cells comprising a glial scar ( ) extending about 200 : m below the tip. One neuron shows a weak NeuN stain (**=>**). NeuN-peroxidase immunoreaction with Nissl counter stain.

Figure 10. SP131, Track of stabilizing shank 1. This section shows a portion of the thick capsule surrounding the track (Tr). The capsule is composed of glial cells and fibroblasts that have grown

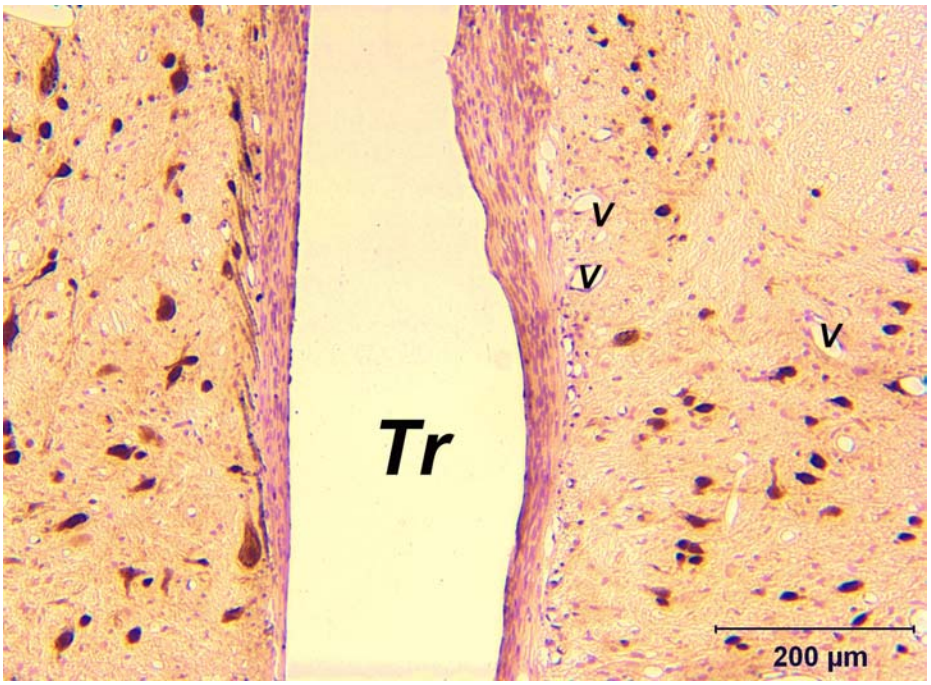

along and down the side of the stabilizing shank. Adjacent to the capsule are blood vessels (v), and brown-colored, NeuN-positive neurons and their processes. NeuN-peroxidase immunoreaction with Nissl counter stain.

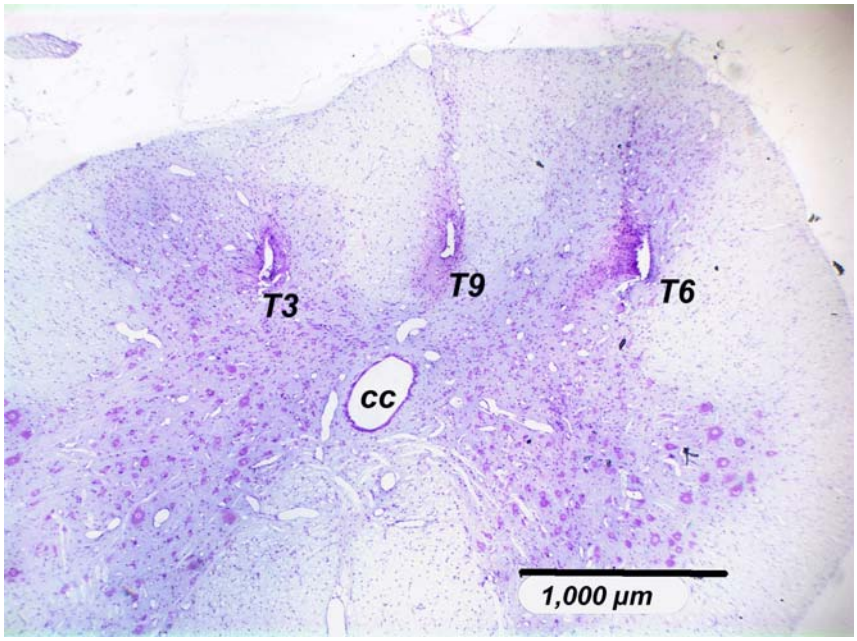

Figure 11. SP132, Tracks of E3, E6 and E9. This low magnification view shows a section several microns rostral to the electrode tips (T_n). The central canal (CC) is also shown. Nissl stain.

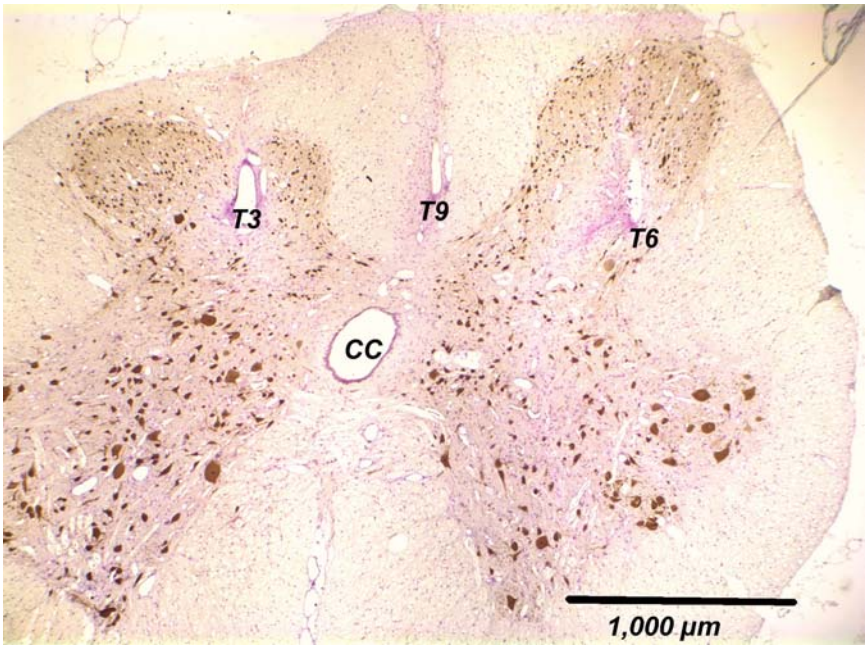

Figure 12. SP132, E3, E6 and E9. This section is 8 ：m rostral to the Nissl stained section shown in Figure 11, and shows the extent of altered regions immediately surrounding the electrodes tracks. The central canal (CC) is also shown. The region is well delineated by the combination of the NeuN stain and Nissl counter-stain.

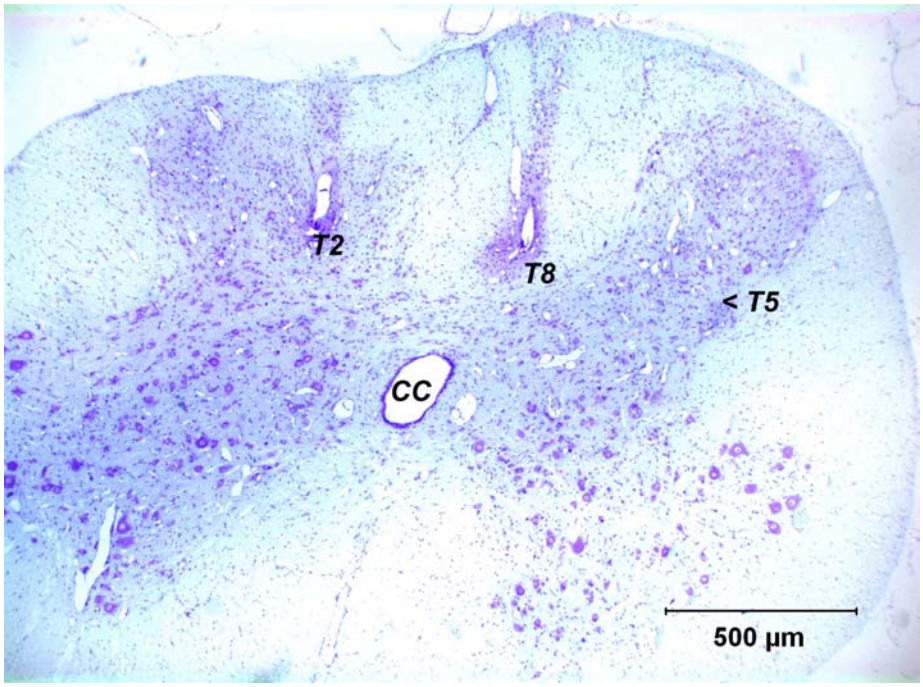

Figure 13. SP132, E2, E5 , E8. This section shows the approximate tip sites (Tn) of E2 and E8, and an area close to the tip site of E5 (**>**), which is located in an adjacent section. The central canal (CC) is also shown. Nissl stain.

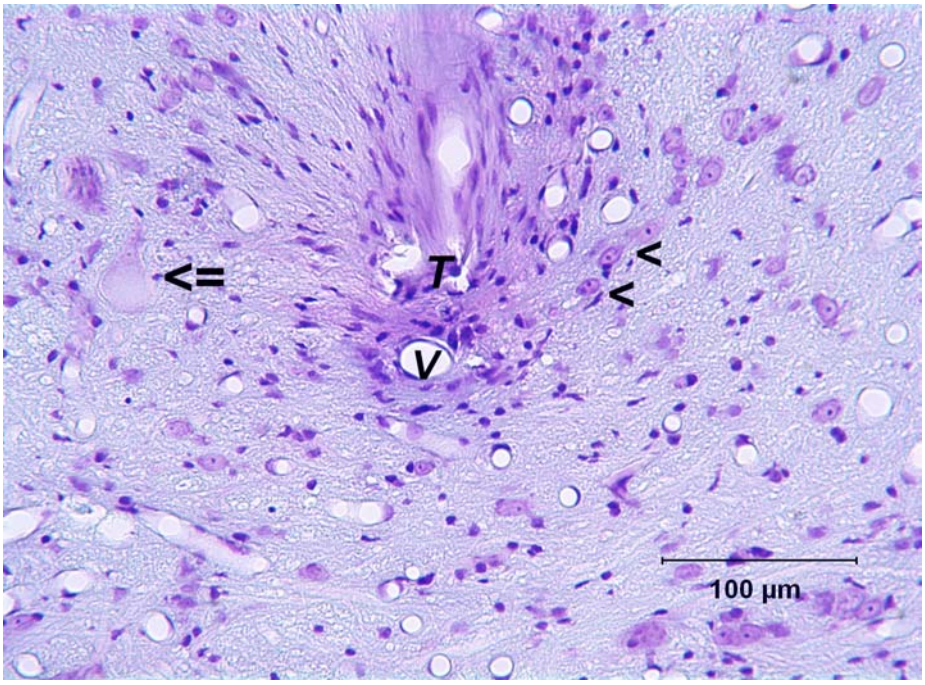

Figure 14. SP132, E2. This section shows the electrode tip site (T) without a gliotic scar ventral to the tip. Note several vessels (v), normal appearing neurons (**<**) and a single neuron expressing chromatolysis with an eccentric nucleus (**<=**). Nissl stain.

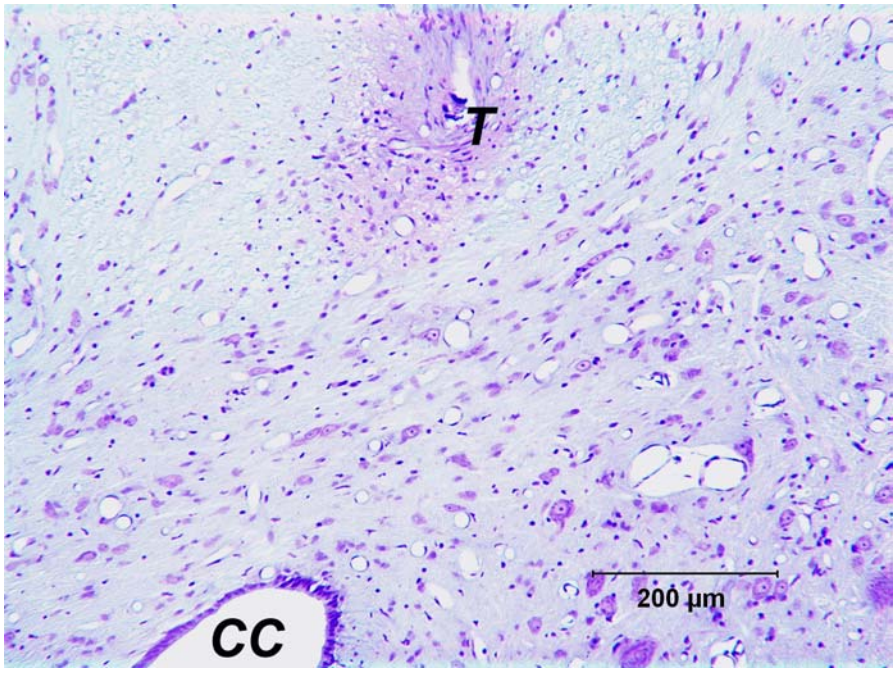

Figure 15. SP132, E8. This section shows the relation between the electrode tip site (T) and the central canal (CC). Nissl stain.

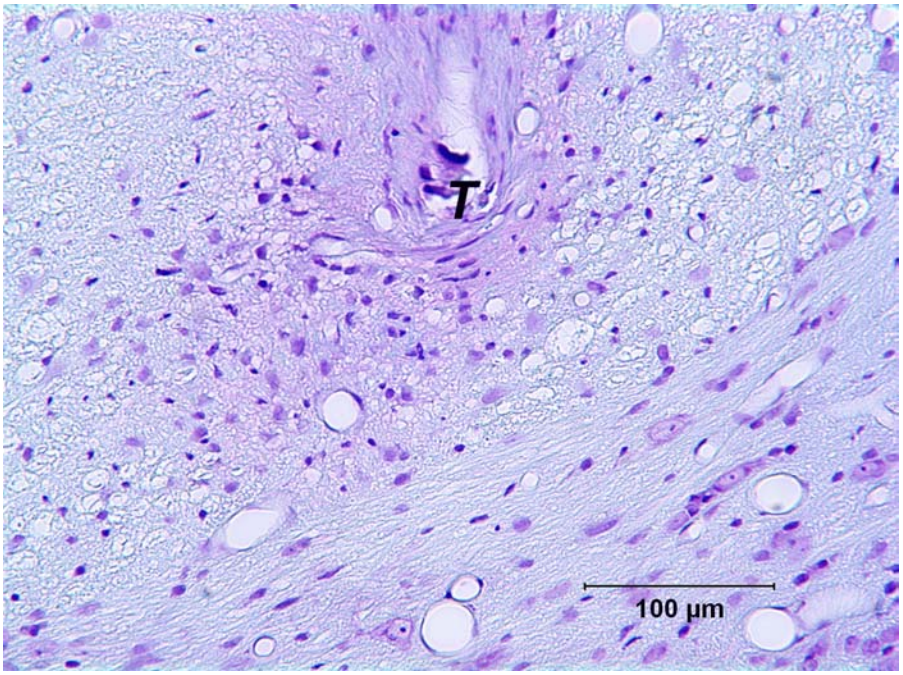

Figure 16. SP132, E8. This section shows a higher magnification of the electrode tip site (T). There is no gliotic scar ventral to the tip site. Nissl stain.

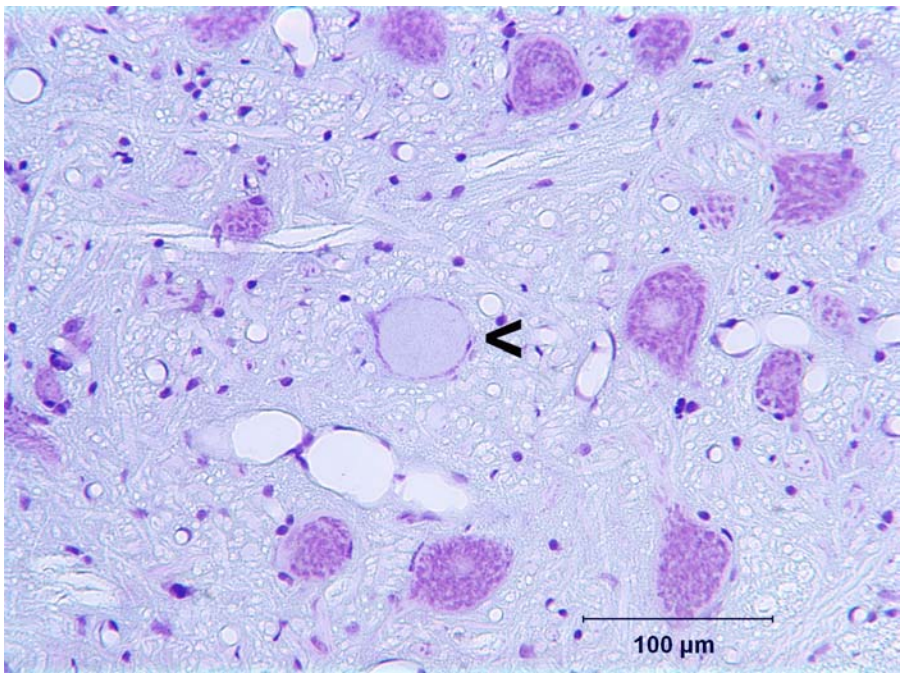

Figure 17A, SP132. This section shows a portion of the ventral horn with large motor neurons stained with Nissl. Note the single neuron expressing chromatolysis changes (**<**), also noted in Figure17B. Nissl stain.

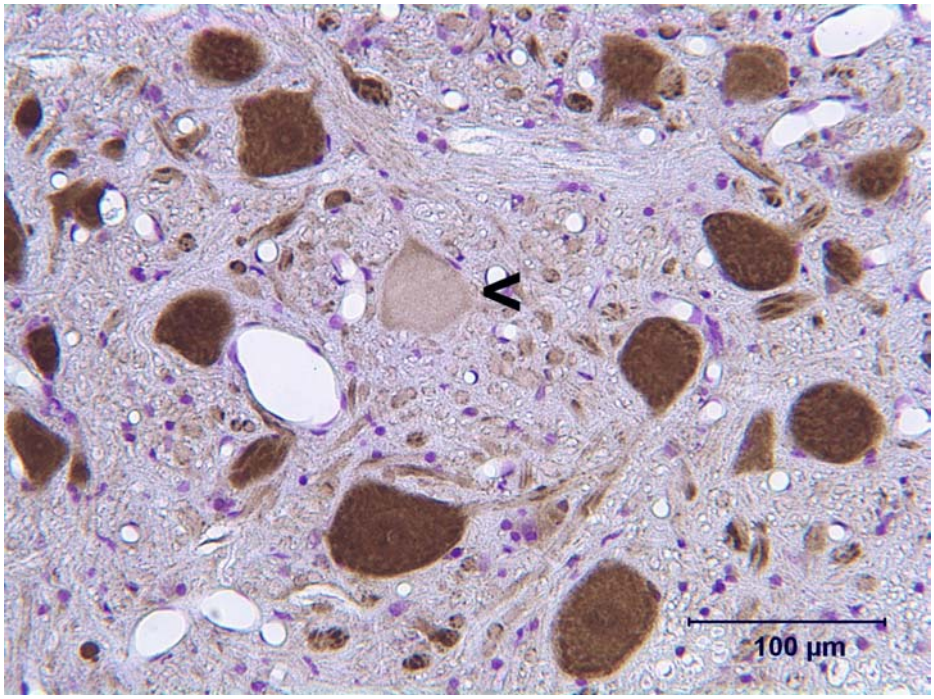

Figure 17B. SP132. This section is 16 ：m rostral of the one shown in figure 17A, and shows the same chromatolytic neuron (**<**) stained with Neun and counter stained with Nissl. Figure 17A and 17B suggest that some neurons that have sustained injury will stain less strongly for the NeuN protein. NeuN-peroxidase immunoreaction with Nissl counter stain.